

# Efficient Photodetection at IR Wavelengths by Incorporation of PbSe–Carbon-Nanotube Conjugates in a Polymeric Nanocomposite\*\*

By Namchul Cho, Kaushik Roy Choudhury, Ram B. Thapa, Yudhithira Sahoo, Tymish Ohulchanskyy, Alexander N. Cartwright, Kwang-Sup Lee,\* and Paras N. Prasad\*

Polymeric nanocomposites have demonstrated great potential for the construction of physically flexible, large-area optoelectronic devices that can remain photoactive over a wide spectral bandwidth, depending on the customizable constituents. They bolster the prospect of developing ultrafast, sensitive, and superior optical counterparts of the corresponding electronic devices. With the successful integration of inorganic quantum dots (QDs) into conjugated polymeric matrices,<sup>[1]</sup> efficient photodetection in different ranges of the electromagnetic spectrum has already been realized.<sup>[2]</sup> This is enabled by the tunable optical absorption and emission of the QDs (by virtue of quantum size effects),<sup>[3]</sup> and also by the fact that the QDs can often preserve their optoelectronic integrity within a host matrix. To generate excitons at a good quantum efficiency, the QDs should have an appreciable absorption cross section at the excitation wavelength.<sup>[4]</sup> The photogenerated excitons should disintegrate into free charge carriers at higher rate than competitive exciton recombination. Subsequently, these charge carriers should be extracted from the photoconverter before relaxation. To realize efficient photon conver-

sion, the rates of photogenerated-carrier separation, interfacial transfer across the different contacts, transport through the matrix, and subsequent collection at the electrodes must all be fast enough compared to exciton recombination.<sup>[5]</sup> Therefore, it is imperative to provide an efficient transport of charges within the nanocomposite by incorporating compatible constituents that facilitate the transport process.

In research on photoconducting devices that use conjugated polymers, electron-accepting materials such as C<sub>60</sub> and single-walled carbon nanotubes (SWNTs) have been utilized in some of the past studies.<sup>[6]</sup> SWNTs are fascinating materials because of several peculiar physical properties. Envisioned as a rolled-up graphene sheet capped with fullerene-like structures, a SWNT can behave as a metal or semiconductor as a function of the wrapping angle of the sheet and the diameter of the nanotube.<sup>[6,7]</sup> In the “metallic” state,<sup>[8]</sup> SWNTs are good ballistic conductors with a reported current density at least one order of magnitude higher than that of copper wires with the same diameter.<sup>[9]</sup> Because of their good mechanical properties (high elastic modulus and high optical transparency), SWNTs have been used for constructing large-area transmissive films,<sup>[10]</sup> making them an ideal component for electrical coupling in futuristic photonic devices.

The aim of the current study is to investigate the photodetection efficiency of a polymeric nanocomposite containing IR-active PbSe QDs and conducting SWNTs that are chemically attached to each other by a novel procedure. PbSe QDs, endowed with a large Bohr radius, exhibit excellent quantum size effects and can be tuned to a precisely targeted absorption wavelength in the IR region. Therefore, a stable SWNT–PbSe conjugate (by chemical bonding of both components) is a promising candidate for the realization of efficient optoelectronic behavior. The large interfaces in the SWNT–PbSe conjugate offer a tremendous opportunity for efficient exciton dissociation after photogeneration in the PbSe QDs. Efficient dissociation and charge transfer depend on the differences in potential energy and electron affinity between the photoactive species (PbSe QDs) and the other components. As can be seen in Scheme 1, the band alignments with a higher electron affinity than SWNTs allow a nonactivated electron transfer from PbSe QDs to SWNTs.<sup>[11]</sup> Because the ionization potential of the polymer (PVK: poly(vinyl carbazole))<sup>[12]</sup> lies closer to the value for a vacuum than that of the QDs,<sup>[13]</sup> the transfer of photogenerated holes to the polymer also proceeds without

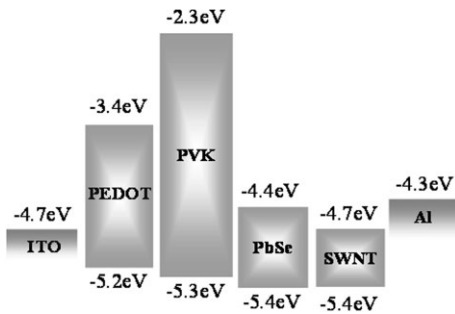
[\*] Prof. K.-S. Lee, N. Cho  
Department of Polymer Science and Engineering  
Hannam University  
Daejeon 306-791 (Korea)  
E-mail: kslee@hannam.ac.kr

Prof. K.-S. Lee, N. Cho  
Institute for Lasers, Photonics and Biophotonics  
University at Buffalo, The State University of New York  
Buffalo, NY 14260-4200 (USA)

Prof. P. N. Prasad, Dr. K. Roy Choudhury, Dr. Y. Sahoo,  
Dr. T. Ohulchanskyy  
Departments of Chemistry and Physics, and  
Institute for Lasers, Photonics and Biophotonics  
University at Buffalo, The State University of New York  
Buffalo, NY 14260-4200 (USA)  
E-mail: pnprasad@buffalo.edu

R. B. Thapa, Prof. A. N. Cartwright  
Department of Electrical Engineering, and  
Institute for Lasers, Photonics and Biophotonics  
University at Buffalo, The State University of New York  
Buffalo, NY 14260-4200 (USA)

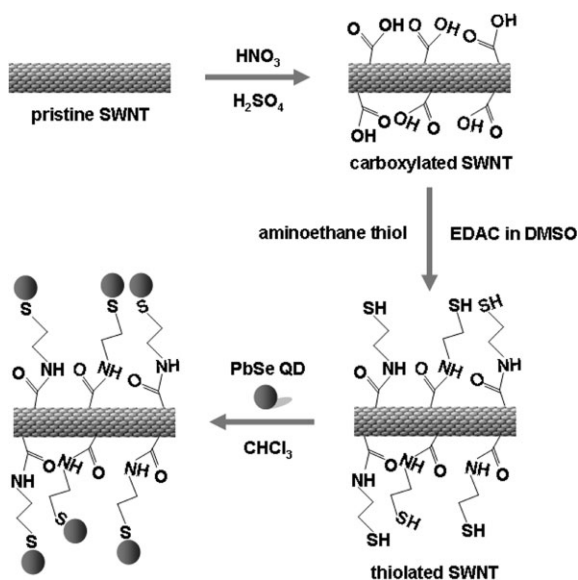
[\*\*] This research was financially supported by the Korea Research Foundation (KRF-2005-013-C00033) and the Asian Office of Aerospace Research and Development (AOARD) (USA). The work at the State University of New York at Buffalo was supported by a Defense University Research Initiative on Nanotechnology Grant through the Air Force Office of Scientific Research (USA).



**Scheme 1.** Energy band diagram for the composite photodetector, indicating the highest occupied molecular orbital–lowest unoccupied molecular orbital (HOMO–LUMO) levels of poly(vinyl carbazole) (PVK), bulk PbSe, and SWNTs, and the work functions of indium tin oxide (ITO), poly(3,4-ethylenedioxythiophene):poly(styrenesulfonate) (PEDOT/PSS), and Al, relative to a vacuum.

a need for any activation energy. The free carriers are transported within the composite matrix by a dc conduction process. Due to the high aspect ratio of the SWNTs, even a moderate loading level in the composite is enough to establish a conducting percolation network, in which the ballistic transport mechanism in SWNTs promotes a high electron mobility, leading to enhanced photocurrents.<sup>[14]</sup>

For efficient charge transfer, it is desirable that the PbSe QDs are intimately attached on the surface of SWNTs, and in high concentration. As shown in Scheme 2, this has been achieved by a novel procedure. The surface of the SWNTs was thiolated before adsorbing the PbSe QDs. We find that the introduction of thiol functional groups on the SWNT surface allows the surface adsorption of PbSe QDs at a density significantly higher than that reported in the literature.<sup>[15]</sup> For this purpose, the SWNTs were first carboxylated and later thiolated by binding a bilinker molecule (2-aminoethanethiol:



**Scheme 2.** Synthetic route for the preparation of SWNTs coupled with PbSe. (EDAC: *N*-(3-dimethylaminopropyl)-*N*-ethylcarbodiimide hydrochloride, DMSO: dimethyl sulfoxide.)

AET) through an amide bond. The SWNT–COOH bond, when activated by *N*-(3-dimethylaminopropyl)-*N*-ethylcarbodiimide hydrochloride (EDAC), easily allows nucleophilic attack of the amine group of AET, resulting in the formation of an amide bond as well as a terminal thiol group on the SWNT (SWNT–SH).<sup>[16]</sup> The attachment between SWNT–SH and PbSe QDs is maximized (because of the large number of available thiol groups) without compromising the colloidal stability of the QDs, thus ensuring their homogeneous sequestration in the polymer.

For the structural characterization, the carboxylation and thiol-group functionalization of the SWNTs were confirmed by Fourier transform IR (FTIR) studies, as shown in Figure 1. The pristine SWNTs have no characteristic bands,<sup>[17]</sup> but a clear C=O stretching vibration at 1724 cm<sup>-1</sup> appears in the

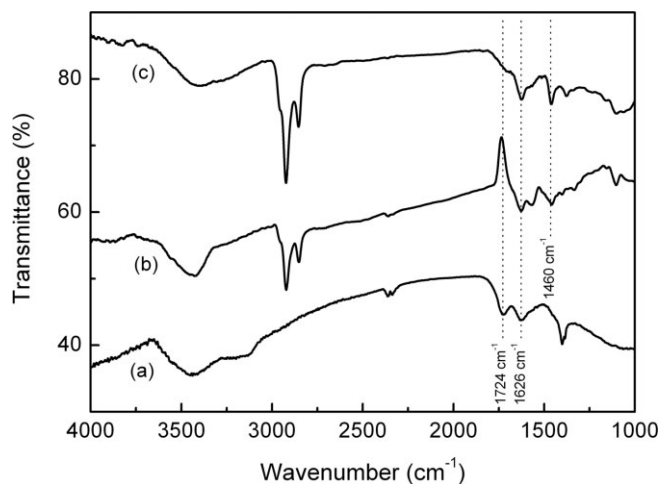


**Figure 1.** a–c) FTIR spectra of SWNT–COOH, SWNT–SH, and SWNT–PbSe, respectively.

spectrum of the carboxylated SWNTs (see Fig 1a).<sup>[18]</sup> The broad band between 3000 and 3600 cm<sup>-1</sup> is a result of O–H absorptions from the carboxylic acid groups. On formation of the amide bond, the carbonyl peaks for both SWNT–SH and SWNT–PbSe shift to 1626 cm<sup>-1</sup> (Fig. 1b and c). Aliphatic C–H stretching (around 2800–2900 cm<sup>-1</sup>) and bending (1460 cm<sup>-1</sup>) correspond to the alkyl group of AET.<sup>[19]</sup> Also, the broad absorption peak near 3400 cm<sup>-1</sup> is indicative of the N–H absorption in the amide bond along with O–H stretching.

The absorption spectra (shown in Fig. 2) of the PbSe samples show the most prominent first excitonic transition, with a peak at 1340–1350 nm and a band edge at 1464 nm, corresponding to a bandgap ( $E_g$ ) value of 0.85 eV, followed by relatively weaker second and third peaks at 1050–1060 nm and 820–830 nm. The absorption peak of SWNT–COOH at 1000 nm is attributed to electronic transitions between different electronic density of states (DOS) configurations corresponding to Van Hove singularities.<sup>[20]</sup> Analysis of SWNT–PbSe indicates that the absorption features of PbSe are suppressed in the conjugate, although the concentration of

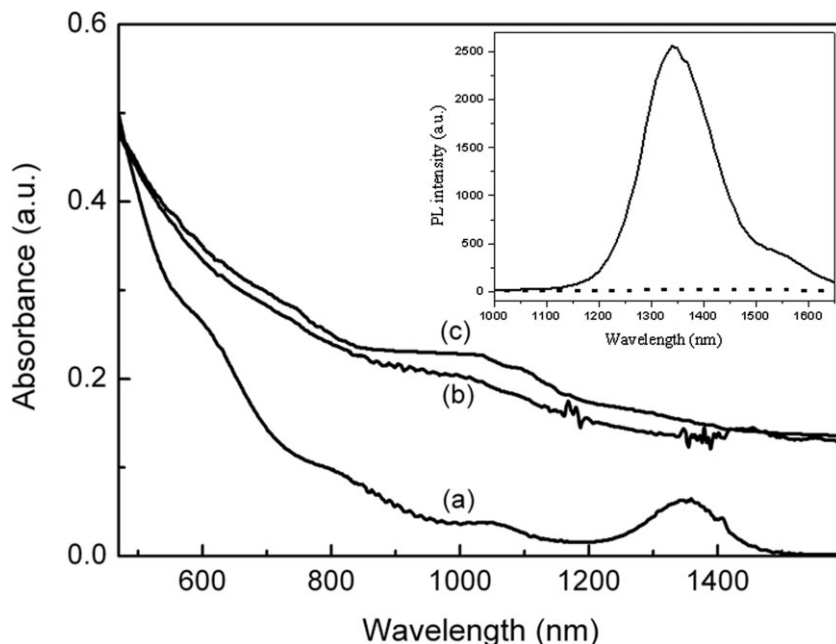


**Figure 2.** a–c) Absorption spectra of PbSe QDs, SWNT–COOH, and SWNT–PbSe, respectively. Inset: Photoluminescence (PL) spectra of colloidal suspensions of PbSe QDs (solid line) and SWNT–PbSe (dotted line) in tetracholoethylene, excited with a 488 nm laser light. The concentration of the PbSe QDs was the same in both cases.

PbSe QDs in both the neat PbSe sample and the SWNT–PbSe conjugate was similar. There is no significant difference between the spectra of the SWNTs and the SWNT–PbSe conjugate (Fig. 2). Suppression of PbSe excitonic features can mean that the quantum confinement conditions for the excitons in the PbSe QDs are compromised when the QDs remain in close proximity with each other and the SWNT, where an overlap of wave functions is highly probable. The results of photoluminescence (PL) measurements agree with this interpretation (Fig. 2, inset). Pure PbSe nanoparticles show intense PL, with a peak at ca. 1350 nm (solid line in inset of Fig. 2) that corresponds to the first excitonic absorption band. A substantial decrease in the PL intensity (more than 1000-fold) was observed for the SWNT–PbSe sample (dotted line in inset of Fig. 2). A supra-assembly of QDs has been shown to exhibit a transition to an extended electronic state, analogous to the Anderson transition in disordered solids, resulting in the suppression of excitonic features, as observed for CdSe QDs in a thin-film configuration.<sup>[21]</sup> Such a reasoning can partially account for the diminished PL, but it is also highly likely that an appreciable and swift electron transfer from the PbSe QDs to the SWNT is facilitated, resulting in the dramatic decrease in PL shown in the inset of Figure 2.

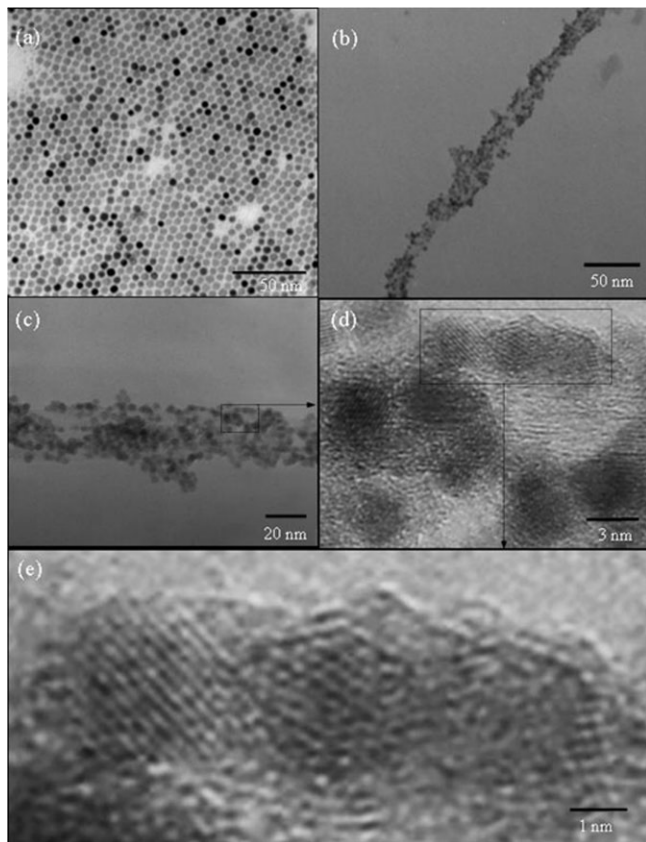
The PbSe QDs (ca. 4 nm) used to prepare the conjugate are extremely monodisperse (Fig. 3a) and orientate into an ordered hexagonal superlattice when the surface is hydrophobic. Examination of transmission electron microscopy (TEM) images of the SWNT–PbSe conjugate (Fig. 3b) reveals that a large number of PbSe QDs bind to the terminal thiol groups

of the SWNTs. Figure 3c–e shows magnifications of a SWNT–PbSe conjugate, where single strands of SWNTs in the SWNT bundles as well as the lattice fringes of PbSe are discernible.

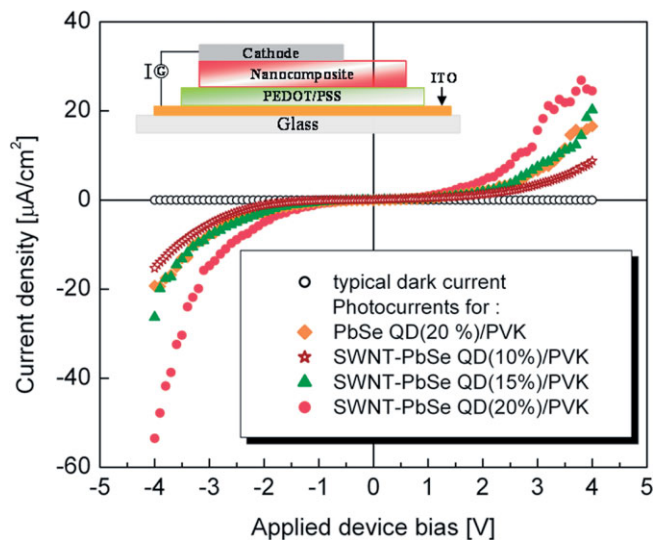
Composite dispersion of the constituents was performed by combining appropriate proportions of PVK and the SWNT–PbSe complex in chloroform, followed by homogenization via vigorous stirring and ultrasonication. A 50 nm thick layer of PEDOT/PSS (PEDOT: poly(3,4-ethylenedioxythiophene); PSS: poly(styrenesulfonate); Baytron-P) was spin-cast onto indium tin oxide (ITO) substrates to improve charge transport through the device. This was followed by spin-casting the active layer of the photodetector from the composite solution. The resulting samples (with an average thickness of 500–600 nm) were dried overnight in vacuum to ensure complete solvent removal. Finally, aluminum counter electrodes were thermally evaporated through a standard shadow mask under high vacuum to yield a sandwichlike device with an active area of ca. 0.04 cm<sup>2</sup> (see inset of Fig. 4).

Figure 4 shows the measured dark currents and photocurrents in two different sets of composite devices. In one set, consisting of the PbSe-QD/PVK composites, the photocurrent increases significantly as a function of the loading fraction of QDs. Pure PVK has a negligible absorption at wavelengths longer than 370 nm, and no photoresponse was obtained on 1340 nm excitation when only PVK was used. Hence, the increased photocurrent indicates quantitative IR sensitization of the polymer by the QDs.<sup>[22]</sup>

In the set of devices containing the SWNT–PbSe complex, the photocurrent was enhanced even further compared to the first set containing just the QDs. Figure 4 shows the results of devices with different loading levels (expressed in wt %) of the SWNT–QD conjugate in the composite. It was noted that for devices containing the SWNT–PbSe conjugate, the photocurrent is larger per effective load fraction of the PbSe QDs. For example, the photocurrent at a SWNT–PbSe conjugate loading of 15 wt % surpasses that of 20 wt % load fractions of isolated PbSe QDs. The best performance was obtained from devices with a SWNT–PbSe conjugate loading level of 20 wt %. The photocurrent enhancement factor, compared to devices with an equal loading level of photosensitizing QDs, is more than two at the highest operating bias. The dark currents are less than 10<sup>−7</sup> A for all the measured devices. One important concern for this single-active-layer device is that the SWNT ropes or bundles could potentially short-circuit the electrodes along the thickness of the nanocomposite device, provided: i) a single rope is longer than the thickness of the device, and ii) many ropes form a percolative dc network



**Figure 3.** a) TEM image of ca. 4 nm PbSe QDs employed in this study. b) TEM image of SWNT–PbSe. c) High-resolution TEM (HRTEM) image of SWNT–PbSe. d) Magnified HRTEM image of the area indicated by the square in (c). e) Magnified HRTEM image of the area indicated by the square in (d).



**Figure 4.** Current density–voltage ( $I$ – $V$ ) characteristics of PbSe-QD/PVK and SWNT–PbSe/PVK devices in the dark and under illumination, illustrating the enhancement of photocurrent in the IR with increasing content of the SWNT–PbSe conjugate. Inset: structure of the IR photodetector device employed in this study.

across the thickness. As is observed here, the dark current remains very low, even at the highest applied bias of 4 V (Fig. 4); hence, there is no incident of SWNTs creating a short-circuit in the nanocomposite. This may have been assisted by the centripetal force exerted during spin-casting, which would tend to align the SWNT ropes in the plane of the substrate rather than across the thickness of the device. The orientation of the ropes would also depend on the viscosity of the casting solution, the solvent evaporation rate, and the concentration of the SWNTs. In summary, it is obvious that short-circuiting due to SWNTs is not an issue in our case.

The external quantum efficiency (EQE) of such photodetectors is defined as the ratio of the number of collected charges at the electrode to the number of incident photons at the wavelength of operation. Efficient harvesting of IR photons, followed by fast charge transfer, and enhanced conduction in the polymer and SWNT networks result in a maximum EQE of ca. 2.6 %, obtained in the devices with 20 wt % of SWNT–PbSe. Compared to PbSe-QD/PVK devices (with a similar number of isolated QDs) that exhibit an EQE of ca. 1.2 %, this corresponds to an increment of more than 100 %.

The photoinduced charge generation in a nanocomposite material depends on the efficient capture of electron–hole pairs of the photodissociated exciton before they can recombine and generate photoluminescence. This study shows that by incorporating SWNT–PbSe conjugates, in which a large number of PbSe QDs is attached to the nanotubes, efficient charge separation and transport is achieved. This study combines several distinct merits of the constituents of a polymeric nanocomposite: the highly efficient exciton generation of PbSe QDs, the efficient electron transfer to SWNT resulting from intimate and high-density attachment of QDs, the low-percolation-threshold dc conduction path due to the SWNTs, and above all a ballistic transport mechanism in the SWNTs, all of which lead to a considerable enhancement of photocurrent over and above a device without the SWNT constituent.

## Experimental

**Sample Preparation:** PbSe QDs were prepared according to a method reported earlier [22]. Briefly, PbO (5 mmol) and oleic acid (25 mmol) were added to 20 mL of tri-*n*-octylamine. The reaction mixture was heated under alternate vacuum and argon atmospheres for 30 min at 155 °C, after which 10 mL of 1 M selenium dissolved in tri-*n*-octylphosphine (TOP-Se) was rapidly injected into the reaction flask. A monodispersed crop of PbSe QDs was formed by this reaction, which could be retrieved at different size fractions. The QDs were cleaned of excess surfactant, oleic acid, and other side products by repeated washing with excess acetone and centrifugation.

The procedure of attaching PbSe QDs onto SWNT is given below: First, the SWNT (bundles with diameter 1.2–1.5 nm and length 2–5 µm, Aldrich, 50 %) surface was carboxylated by oxidation with a mixture of H<sub>2</sub>SO<sub>4</sub>/HNO<sub>3</sub>. SWNTs (80 mg) were stirred in 40 mL of H<sub>2</sub>SO<sub>4</sub>/HNO<sub>3</sub> (3:1) solution for 24 h at room temperature (RT). The reaction mixture was centrifuged and washed with water several times to remove the excess acid. 160 mg of EDAC was added to the carboxylated SWNT (SWNT–COOH) in DMSO to activate the carboxyl

group, followed by the addition of 500 mg of AET and stirring for 12 h at room temperature. After the coupling reaction with AET, excess EDAC and AET were removed by centrifuging and washing with DMSO and acetone. The precipitate was sonicated in chloroform to obtain a stable dispersion.

The surface of PbSe QDs was stripped of a fraction of the oleic acid monolayer by washing with excess ethanol and centrifuging. These QDs, with partially bare surfaces, were redispersed in chloroform and subsequently SWNT-SH was stirred in with them. The mixture was stirred for 12 h in chloroform. Any free PbSe was separated by centrifuging with microcentrifuge filters (molecular weight cut-off 100 000 Da PTHK polysulfone membrane, Aldrich), and the product SWNT-PbSe in the residue was redispersed in chloroform.

**Sample Characterization:** Absorption spectra were recorded using a Shimadzu 3101PC spectrophotometer. A SPEX 270M spectrometer (Jobin Yvon) equipped with an InGaAs photodetector (Electro-Optical Systems Inc., USA) was used for acquisition of PL emission spectra. An argon ion laser (BeamLok, Spectra-Physics, 488 nm line) was used for PL excitation. The same excitation power was maintained for every round of acquisition. The samples in quartz cuvettes were mounted directly in front of the entrance slit of the spectrometer, and the exciting laser beam was directed at 90° relative to the collection of emission.

FTIR spectra of carboxylated SWNT, thiolated SWNT, and SWNT-PbSe conjugates in KBr pellets were obtained. These measurements were made using a Perkin-Elmer FTIR spectrometer model 1760X operating in transmission mode. Transmission electron microscopy (TEM) images were obtained with a Model 200 JEOL microscope at an acceleration voltage of 200 kV. The specimens were prepared by drop-casting a dispersion of the sample in chloroform onto an amorphous-carbon-coated 300 mesh copper grid.

**Device Fabrication:** ITO-coated glass substrates were cleaned with detergent, followed by ultrasonication sequentially in acetone, ethanol, isopropyl alcohol, and dried in a vacuum oven. A 50 nm layer of PEDOT/PSS was spin-coated from aqueous solution. PVK was dissolved in chloroform to make a 10 mg mL<sup>-1</sup> solution. To this, either solitary QDs of PbSe or the SWNT-PbSe conjugate was added in various proportions, and the mixture homogenized thoroughly. Thin-film devices were spin-coated at 1000 rpm to yield 500–600 nm thick samples, which were dried in a vacuum oven overnight to ensure complete solvent removal. Aluminum counter electrodes were thermally evaporated to get the final device structure.

**I-V Characterization:** The current-voltage characteristics in dark and under illumination were measured with a Keithley Sourcemeter interfaced with Labview software for data acquisition. The devices were optically excited by a continuous-wave semiconductor laser operating at 1340 nm.

Received: March 27, 2006

Revised: August 17, 2006

- [1] a) N. C. Greenham, X. Peng, A. P. Alivisatos, *Phys. Rev. B: Condens. Matter Mater. Phys.* **1996**, *54*, 17628. b) D. S. Ginger, N. C. Greenham, *Phys. Rev. B: Condens. Matter Mater. Phys.* **1999**, *59*, 10622. c) W. U. Huynh, J. J. Dittmer, A. P. Alivisatos, *Science* **2002**, *295*, 2425. d) D. Selmarten, M. Jones, G. Rumbles, P. Yu, J. Nedeljkovic, S. Shaheen, *J. Phys. Chem. B* **2005**, *109*, 15927.
- [2] a) D. Qi, M. Fischbein, M. Drndic, S. Šelmic, *Appl. Phys. Lett.* **2005**, *86*, 093103. b) S. A. McDonald, G. Konstantatos, S. Zhang, P. W. Cyr, E. J. D. Klem, L. Levina, E. H. Sargent, *Nat. Mater.* **2005**, *4*, 138. c) A. Maria, P. W. Cyr, E. J. D. Klem, L. Levina, E. H. Sargent, *Appl. Phys. Lett.* **2005**, *87*, 213112. d) K. R. Choudhury, Y. Sahoo, P. N. Prasad, *Adv. Funct. Mater.* **2005**, *15*, 751.
- [3] a) J. S. Steckel, S. Coe-Sullivan, V. Bulovic, M. Bawendi, *Adv. Mater.* **2003**, *15*, 1862. b) L. Bakueva, S. Musikhin, M. A. Hines, T.-W. F. Chang, M. Tzolov, G. D. Scholes, E. H. Sargent, *Appl. Phys. Lett.* **2003**, *82*, 2895.
- [4] R. J. Ellingson, M. C. Beard, J. C. Johnson, P. Yu, O. I. Micic, A. J. Nozik, A. Shabaev, A. L. Efros, *Nano Lett.* **2005**, *5*, 865.
- [5] A. J. Nozik, *Inorg. Chem.* **2005**, *44*, 6893.
- [6] a) G. Yu, J. Gao, J. C. Hummelen, F. Wudl, A. J. Heeger, *Science* **1995**, *270*, 1789. b) J. J. M. Halls, K. Pichler, R. H. Friend, S. C. Moratti, A. B. Holmes, *Appl. Phys. Lett.* **1996**, *68*, 3120. c) P. P. Neupane, M. O. Manasreh, B. D. Weaver, R. P. Rafaelle, B. J. Landi, *Appl. Phys. Lett.* **2005**, *86*, 221908. d) G. M. A. Rahman, D. M. Guldi, R. Cagnoli, A. Mucci, L. Schenetti, L. Vaccari, M. Prato, *J. Am. Chem. Soc.* **2005**, *127*, 10051. e) E. Kymakis, I. Alexandrou, G. A. J. Amaratunga, *J. Appl. Phys.* **2003**, *93*, 1764.
- [7] T. W. Odom, J.-L. Huang, P. Kim, C. M. Lieber, *Nature* **1998**, *391*, 62.
- [8] a) S. Frank, P. Poncharal, Z. L. Wang, W. A. de Heer, *Science* **1998**, *280*, 1744. b) A. Bachtold, M. S. Fuhrer, S. Plyasunov, M. Forero, E. H. Anderson, A. Zettl, P. L. McEuen, *Phys. Rev. Lett.* **2000**, *84*, 6082. c) A. Thess, R. Lee, P. Nikolaev, H. Dai, P. Petit, J. Robert, C. Xu, Y. H. Lee, S. G. Kim, D. T. Colbert, G. Scuseria, D. Tománek, J. E. Fischer, R. E. Smalley, *Science* **1996**, *273*, 483.
- [9] a) R. V. Seidel, A. P. Graham, P. Rajasekharan, E. Unger, M. Liebau, G. S. Duesberg, F. Kreupl, W. Honlein, *J. Appl. Phys.* **2004**, *96*, 6694. b) F. Kreupl, A. P. Graham, G. S. Duesberg, W. Steinhögl, M. Liebau, E. Unger, W. Honlein, *Microelectron. Eng.* **2002**, *64*, 399.
- [10] Z. Wu, Z. Chen, X. Du, J. M. Logan, J. Sippel, M. Nikolou, K. Kamaras, J. R. Reynolds, D. B. Tanner, A. F. Hebard, A. G. Rinzler, *Science* **2004**, *305*, 1273.
- [11] a) S. Kazaoui, N. Minami, N. Matsuda, H. Kataura, Y. Achiba, *Appl. Phys. Lett.* **2001**, *78*, 3433. b) B. J. Landi, S. L. Castro, H. J. Ruf, C. M. Evans, S. G. Bailey, R. P. Raffaele, *Sol. Energy Mater. Sol. Cells* **2005**, *87*, 733.
- [12] S. Chaudhary, M. Ozkan, W. C. W. Chan, *Appl. Phys. Lett.* **2004**, *84*, 2925.
- [13] S. E. Kohn, P. Y. Yu, Y. Peroff, Y. R. Shen, Y. Tsang, M. L. Cohen, *Phys. Rev. B: Condens. Matter Mater. Phys.* **1973**, *8*, 1477.
- [14] E. Kymakis, G. A. J. Amaratunga, *Appl. Phys. Lett.* **2002**, *80*, 112.
- [15] a) J. Liu, A. G. Rinzler, H. Dai, J. H. Hafner, R. K. Bradley, P. J. Boul, A. Lu, T. Iverson, K. Shelimov, K. Huffman, F. Rodriguez-Macias, Y.-S. Shon, T. R. Lee, D. T. Colbert, R. E. Smalley, *Science* **1998**, *280*, 1253. b) S. Banerjee, S. S. Wong, *Nano Lett.* **2002**, *2*, 195. c) J. M. Haremza, M. A. Hahn, T. D. Krauss, S. Chen, J. Calcines, *Nano Lett.* **2002**, *2*, 1253.
- [16] P. Schuets, F. Caruso, *Adv. Funct. Mater.* **2003**, *13*, 929.
- [17] P. He, M. W. Urban, *Biomacromolecules* **2005**, *6*, 2455.
- [18] J. Chen, M. A. Hamon, H. Hu, Y. Chen, A. M. Rao, P. C. Eklund, R. C. Haddon, *Science* **1998**, *282*, 95.
- [19] Y. Qin, L. Liu, J. Shi, W. Wu, J. Zhang, Z.-X. Guo, Y. Li, D. Zhu, *Chem. Mater.* **2003**, *15*, 3256.
- [20] a) T. Pichler, M. Knupfer, M. S. Golden, J. Fink, A. Rinzler, R. E. Smalley, *Phys. Rev. Lett.* **1998**, *80*, 4729. b) O. Jost, A. A. Gorbunov, W. Pompe, T. Pichler, R. Friedlein, M. Knupfer, M. Reibold, H.-D. Bauer, L. Dunsch, M. S. Golden, J. Fink, *Appl. Phys. Lett.* **1999**, *75*, 2217.
- [21] M. V. Artemyev, A. I. Bibik, L. I. Gurinovich, S. V. Gaponenko, H. Jaschinski, U. Woggon, *Phys. Status Solidi B* **2001**, *224*, 393.
- [22] K. R. Choudhury, Y. Sahoo, T. Y. Ohulchanskyy, P. N. Prasad, *Appl. Phys. Lett.* **2005**, *87*, 073110.